Modulation of Nuclear Pore Topology by Transport Modifiers

Rainer D. Jäggi,* Alfredo Franco-Obregón,* Petra Mühlhäusser,† Franziska Thomas,† Ulrike Kutay,† and Klaus Ensslin*

*Solid State Physics Laboratory, ETH Zürich, 8093 Zürich, Switzerland and †Institute of Biochemistry, ETH Zürich, 8093 Zürich, Switzerland

ABSTRACT The nuclear pore complex (NPC) represents the only pathway for macromolecular communication between the nuclear and cytoplasmic compartments of the cell. Nucleocytoplasmic transport requires the interaction of transport receptors with phenylalanine–glycine (FG)-repeats that line the transport pathway through the NPC. Here we examine the effects of transport receptors and amphipathic alcohols on NPC topology using scanning force microscopy. We show that transport receptors that irreversibly bind FG-repeats increase NPC vertical aspect, whereas transport receptors that weakly interact with FG-repeats increase NPC diameter. Interestingly, small polar alcohols likewise increase NPC diameter. These opposing effects agree with the inhibition or enhancement of nuclear transport, respectively, previously ascribed to these agents.

INTRODUCTION

Nuclear pores are one of the largest protein complexes present in the cell. The nuclear pore complex (NPC) has a molecular mass of 125 MDa and comprises some 30–50 different proteins, or nucleoporins, that are expressed in multiple copies (reviewed in Görlich and Kutay, 1999). Because of its large size and high density on the nuclear envelope, the NPC was one of the first biological macromolecular complexes to be examined with scanning force microscopy (SFM) in amphibian (Perez-Terzic et al., 1996; Stoffler et al., 1999; Wang and Clapham, 1999; Danker and Oberleithner, 2000) and mammalian cells (Oberleithner et al., 1994; Franco-Obregón et al., 2000). Despite the wealth of structural information obtained with this approach, however, little new information was gained concerning classical nuclear transport pathways. Classically, nuclear transport is mediated by transport receptor proteins that chaperone cargo through the NPC after making contacts with specific nucleoporins. Whether cargo translocation via classical pathways is accompanied by conformational changes in NPC structure is still an open question.

Nuclear transport receptors target to the NPC by recognizing particular hydrophobic amino acid residues expressed within specific nucleoporins (Radu et al., 1995; Stewart, 2000). In this respect a common feature of many nucleoporins is phenylalanine–glycine (FG)-repeat motifs. Several lines of evidence indicate that interaction of transport cargo with such FG-repeats is essential for efficient nucleocytoplasmic transport. Specifically, NPCs lacking certain FG-containing nucleoporins no longer support transport (Finlay and Forbes, 1990), antibodies to FG-repeats inhibit nuclear transport (Powers et al., 1997), and FG-nucleoporins immunologically localize to the conduction pathway through the NPC (Grote et al., 1995). Nevertheless, how the interaction between transport complexes and the FG-nucleoporins actually translates into translocation remains enigmatic.

Several nuclear transport pathways have thus far been identified of which the importin-α/β transport complex is the best characterized (Görlich and Kutay, 1999). Here, importin-α mediates cargo binding to importin-β that, via its interactions with FG nucleoporins, targets the intact import complex to the NPC. Binding of importin-β to the FG-repeats is an energetically favored process. Unbinding, on the other hand, requires an auxiliary protein known as Ran, a Ras-related GTPase. More precisely, in the absence of Ran-binding or in the presence of Ran-GDP importin-β freely associates with importin-α/cargo, thus forming an import competent transport complex. On the other hand, importin-β, when bound by Ran-GTP, dissociates from the NPC, thus terminating the transport process. Because the Ran-GTP concentration is greatest within the nucleus, nuclear import is the default direction for this pathway. Predictably, disrupting the Ran-GTP binding domain of importin-β results in irreversible FG-binding that ultimately impedes further transport through the NPC (Kutay et al., 1997). Therefore, although the recognition of FG-repeats by transport receptors is imperative for nuclear transport to take place, lower affinity interactions with FG-repeats should allow more rapid transport of cargo through the NPC, albeit with a loss of specificity.

Here we investigate the influence on NPC topology of mutated transport receptor proteins and amphipathic molecules, which are known to modify nuclear transport properties. We clearly identified changes in the vertical and lateral aspects of NPCs, which are induced either by certain importin-β mutants or by amphipathic alcohols. We were thus able to correlate microscopic changes in NPC topology as discerned with SFM to previously obtained results from biochemical experiments examining nuclear transport.

MATERIALS AND METHODS

Scanning force microscopy

Imaging of nuclear envelope samples was performed with a BioScope AFM (Digital Instruments, Veeco Metrology Group, Santa Barbara, CA) using silicon nitride cantilevers (spring constant 0.16 N/m) with oxide-sharpened tips (Olympus Optical Co., Ltd., Japan). Cantilever tips of this sort typically

Submitted June 3, 2002, and accepted for publication September 30, 2002.

Address reprint requests to Klaus Ensslin, E-mail: ensslin@phys.ethz.ch.

0006-3495/03/01/665/06 $2.00

had tip radii smaller than 20 nm and cone opening angles of 25° (manufacturer's specifications). Fortuitously, SFM images of NPCs (Fig. 1) were amenable for the reconstruction of the actual tip shape. Using the tip qualification feature provided with the Nanoscope III software (Digital Instruments, Veeco Metrology Group, Santa Barbara, CA) or by inspection of profiles across single NPCs (e.g, Fig. 1 *I*) we were able to verify that all tips exhibited similar characteristics. Tip radii determined by these methods were typically smaller than that indicated by the manufacturer, namely <15 nm. Thus, our measurements of NPC lateral and vertical aspects were generally not limited by the tip aspect ratio (see Data analysis). In fact, under optimal conditions, control NPCs with a pore depth of $\sim$40 nm ($\Delta z \approx -40$ nm) were commonly observed, a value greater than the mean value ($\Delta z \approx -20$ nm) establishing the geometrically allowed limit due to the finite tip aspect ratio. Cantilevers were routinely replaced before the commencement of scanning and a single tip (if not dirtied) was used for a given day's control and experimental conditions in alternating order to rule out systematic errors in the measurements. Scanning was conducted in liquids using tapping mode. In this mode the cantilever is oscillated at a set frequency (typically 8 kHz), and the oscillation amplitude serves as a feedback signal to follow surface topography. Because the tip only intermittently touches the surface, lateral forces exerted on the sample are reduced and image resolution is increased (Jäggi et al., 2001). The oscillation amplitude (setpoint) was carefully monitored during imaging to minimize normal forces exerted by the cantilever tip. At typical setpoints, the cantilever oscillated with an amplitude of $\sim$10 nm, which corresponds to 95% of the amplitude of the freely oscillating cantilever, exerting on the sample average forces significantly below 0.5 nN (Jäggi et al., 2001). Scan speed was adjusted to $\sim 2\ \mu$m/s.

Data analysis

Changes in NPC topology were investigated by taking cross-sectional profiles through single NPCs. To minimize artifacts induced by thermal drift the profile measurements were taken along the fast scan direction of the SFM. The NPC topology was characterized by measurements of upper rim diameter (d) and central pore depth (Δz) as indicated in Fig. 1. To this end, maxima and minima values with respect to the vertical dimension on the pore rim and at the location of the central pore depression, respectively, were determined by careful inspection of each profile. The relative distances between maximum and minimum points were analyzed using a numerical procedure to extract the numbers for pore depth and diameter. Measuring pore diameter at the upper rim, rather than at the outer circumference of the NPC, eliminated any uncertainties associated with limited tip asperity. Thus, diameter measurements were independent of the tip radius and aspect ratio. Measured datasets for depth and diameter were well described by single Gaussian distributions. In all cases diameter and depth data are given as

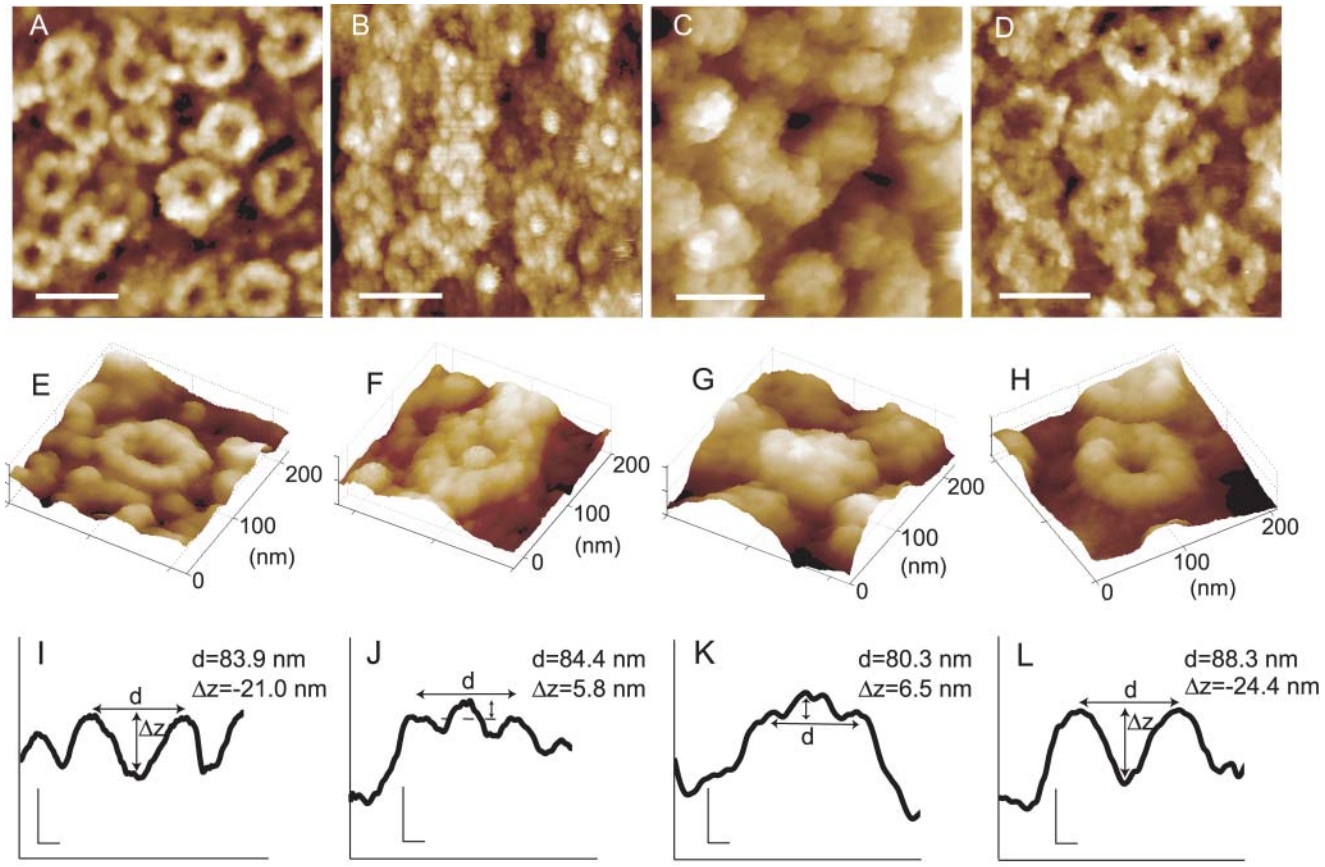

FIGURE 1 Distinct NPC topologies are clearly discerned using scanning force microscopy. SFM images of NPCs that were untreated (*A*, *E*, *I*), subjected to calcium store depletion using 10 mM EGTA for 10 min (*B*, *F*, *J*), incubated in the 45-462 importin-β mutant for 2 min (*C*, *G*, *K*) or treated with 1,2-cyclohexanediol for 2 min (*D*, *H*, *L*). All treatments were performed at 4°C. Scale bars in panels *A–D* represent 200 nm. Panels *E–H* are respective three-dimensional representations of individual NPCs. Panels *I–L* are cross-sectional profiles of the NPCs shown directly above; vertical and horizontal scale bars represent 20 nm. NPC diameter (d) and central channel depth (Δz) were measured as described in the Methods. The 45-462 importin-β mutant lacks functional Ran- and importin-α binding domains. Therefore, changes in NPC topology observed in *C*, *G*, and *K* arise from mutant protein binding over the central channel region leaving the rim of the NPC clearly resolvable.

mean values ±SE. In the figure legends of Figs. 2 and 3, the sample characteristics are given in the format (*a*/*b*/*c*) with *a* indicating the number of individual measurements, *b*, the number of different nuclei analyzed, and *c*, the number of different tips used for a given experimental condition.

Nuclei preparation

Xenopus nuclei were prepared as previously described (Jäggi et al., 2001). Briefly, oocytes were stored (18°C) in Modified Barth's Solution (MBS) consisting of (in mM); 1 KCl, 0.82 $MgSO_4$, 0.41 $CaCl_2$, 0.33 $Ca(NO_3)_2$, 2.4 $NaHCO_3$, 88 NaCl, and 10 HEPES, pH 7.4. Nuclear envelopes were typically prepared for scanning on the day of oocyte isolation. Nevertheless, analogous results could also be obtained on nuclear envelopes from oocytes stored in MBS for up to three days. After dissection, nuclei were immediately transferred into a low salt buffer (LSB) consisting of (in mM): 1 KCl, 0.5 $MgCl_2$, 15 Tris. Nuclei were washed several times in cold (~10°C) LSB to remove any adherent cellular material and debris. After cleaning, nuclei were then transferred to Mock Intracellular Buffer (MIB) consisting of (in mM); 90 KCl, 10 NaCl, 2 $MgCl_2$, 0.75 $CaCl_2$, 1.1 EGTA and 15 Tris, pH 7.32 in which they were incubated in experimental conditions. After incubation in importin-β mutants (1 μM) or amphipathic alcohols (2.0%; Sigma) nuclei were fixed in 2% formaldehyde and 1% glutaraldehyde at 4°C overnight. In preparation for scanning nuclei were placed intact onto plastic tissue culture dishes, partially dried and rehydrated in distilled water. Although initial drying of the nuclear envelope increased the stability of the preparation, undried NPCs exhibited matching dimensions. For example, in the extreme case, untreated, unfixed NPCs scanned without initial drying exhibited pore diameters and depths ($d = 83.3 \pm 0.9$ nm, $\Delta z = -18.3 \pm 0.5$ nm, $n = 47$, respectively) comparable to fixed, dried, and rehydrated samples ($d = 84.9 \pm 0.5$ nm, $\Delta z = -21.1 \pm 0.4$ nm, $n = 425$). Therefore, chemical fixation and partial drying were manners to consistently obtain reproducible results over a broad range of experimental conditions without altering pore dimension. Because the nuclei were imaged intact there was no confusion as to whether imaging was performed on the inner or outer nuclear envelopes.

Molecular biology

The generation, expression, and purification of importin-β and mutant importin-β fragments has been described previously (Kutay et al., 1997; Jäkel and Görlich, 1998; Bayliss et al., 2000). Nuclear envelopes were incubated with importin-β constructs at a concentration of 1 μM in MIB for the indicated times before overnight fixation.

RESULTS AND DISCUSSION

We previously developed a methodology to be used with scanning force microscopy that allowed the accurate measurement of the cytoplasmic features of NPCs with nanometer resolution (Jäggi et al., 2001). Fig. 1 shows examples of SFM images of *Xenopus* oocyte NPCs exhibiting distinct surface topographies. Fig. 1, *A* and *E*, shows untreated NPCs exhibiting the characteristic eightfold symmetry and central channel depression previously described for transport-permissive NPCs (Danker and Oberleithner, 2000; Stoffler et al., 1999). For comparison Fig. 1, *B* and *F*, shows examples of NPCs after depletion of the perinuclear calcium store using EGTA, a pharmacological maneuver previously shown to cause characteristic changes in the NPC conformation that are correlated with a reduction in nuclear permeability (Perez-Terzic et al., 1996). Although the exact origin of the central plug is still a matter of controversy, it is frequently encountered under conditions of calcium store depletion. In support that the plug is a molecular structure particular to calcium depleted envelopes is the finding that the plug can be shown to extrude in real time from untreated (unplugged) NPCs upon the addition of calcium chelators or agents that deplete intracellular calcium reservoirs (Wang and Clapham, 1999).

An example of transport receptor binding is shown in Fig. 1, *C* and *G*, for importin-β fragment 45-462. The 45-462 importin-β lacks part of the N-terminal Ran-binding domain and therefore binds irreversibly to the NPC. Consequently it is a dominant negative blocker of nuclear transport (Kutay et al., 1997). Although this mechanism of transport block implicates steric hindrance rather than changes in NPC conformation per se, NPC topology is nonetheless clearly altered, possibly as the result of the accumulation of bound importin-β molecules over the central region of the NPC.

Amphipathic molecules have been previously shown to functionally abolish NPC selectivity by allowing the unabated entry of larger than normal macromolecules into the nuclear compartment (Ribbeck and Görlich, 2002). Amphipathic alcohols were proposed to exert this effect by effectively competing for hydrophobic interactions with FG-repeats because they could elute a broad range of nuclear transport receptors from a phenyl-Sepharose affinity column. Fig. 1, *D* and *H*, shows examples of NPCs exposed to trans-1,2-cyclohexanediol, one such amphipathic alcohol. Interestingly, central channel diameter is significantly increased in the presence of 1,2-cyclohexanediol. Below each individual NPC image is its corresponding cross-sectional representation depicting the central channel depression characteristic of untreated NPCs (Fig. 1 *I*), the vertical displacement of the central channel translocator after calcium store depletion (Fig. 1 *J*), the binding of the 45-462 mutant protein over the central channel region of the NPC (Fig. 1 *K*), and the increase in NPC diameter induced with 1,2-cyclohexanediol (Fig. 1 *L*). Fig. 1, *I–L*, also gives a diagrammatic description of the diameter and central depth measurements graphically presented later in the paper. We were therefore able to discern distinct NPC conformations that can be correlated with previously described changes in NPC transport capacity using scanning force microscopy.

Modulation in central channel depth

One of the more dramatic changes we observed in NPC topography was the graded change in NPC vertical aspect after incubation with certain importin-β mutants. The effect is graphically represented in Fig. 2 for a variety of importin-β mutants (Kutay et al., 1997; Bayliss et al., 2000; Jäkel and Görlich, 1998) and amphipathic alcohols (Ribbeck and Görlich, 2002). Interestingly, the effect an importin-β mutant construct has on NPC vertical aspect correlates

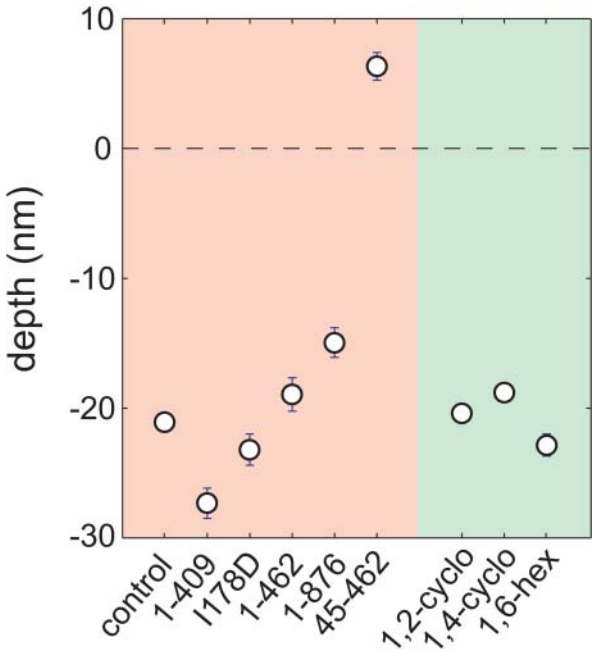

FIGURE 2 Vertical dimension of the NPC after incubation with importin-β constructs (2–10 min) and amphipathic alcohols (2–10 min). Plot of NPC central channel height after incubation with the indicated molecule. Negative values signify depression of the central channel region relative to the cytoplasmic rim of the NPC, whereas positive values indicate a protrusion of the central channel region (see Fig. 1). It is apparent that vertical height of the central channel region steadily increases with higher-affinity binding of importin-β constructs to the NPC (Kutay et al., 1997). In fact, irreversible binding of the 45-462 mutant protein results in the only incidences of central channel protrusion ($0 < \Delta z$). Where not apparent the error bars lie within the dimensions of the symbol. The sample characteristics are as follows: control: (425/21/16), 1-409: (81/2/2), 1-876 I178D: (90/3/3), 1-462: (62/3/3), 1-876: (72/4/3), 45-462: (102/8/8), 1,2-cyclohexanediol: (188/3/2), 1,4-cyclohexanediol: (179/5/5), and 1,6-hexanediol: (109/3/3). See Methods for details.

well with the relative strength of its interactions with FG nucleoporins as described previously (Kutay et al., 1997). On one extreme is the 45-462 importin-β mutant, which irreversibly binds to the NPC and gives rise to a dramatic increase in NPC vertical aspect. On the other extreme is the I178D importin-β mutant, which has its dominant FG-binding domain inactivated and exhibits control-like NPC vertical aspect (Bayliss et al., 2000). Intermediate central channel heights are observed for the 1-462 (importin-α binding domain disrupted) and the 1-876 (full-length importin-β) proteins. Unlike the 45-462 mutants, both these importin constructs have their Ran-binding domains (amino terminals) intact and hence are subject to release from the NPC by Ran-GTP. Interestingly, the 1-409 mutant shows the greatest central channel depth of all importin-β constructs possibly arising from a combination of its relatively small size, weaker binding affinity, and ablation of both importin-α- and BIB-binding domains (Kutay et al., 1997; Jäkel and Görlich, 1998). This result also indicates that the filling of the central channel observed with the wild-type 45-462 mutant is not due to the binding of protein aggregates because the other mutant receptors do not give rise to this effect and yet differ mainly in their NPC binding strengths. Treatment with amphipathic alcohols resulted in NPC pore depths that were virtually indistinguishable from those of controls. Therefore, importin-β constructs that bind with predicted higher affinities accumulate to a greater degree over the central channel area of the NPC in a manner that might act as an impediment to nuclear transport.

Modulation of NPC diameter

Specificity of nuclear transport is dependent upon interactions of transport receptors with FG-nucleoporins. On the one hand, high-affinity binding confers high-specificity. On the other hand, weak FG-binding often translates into increased rates of nuclear transport (Ribbeck and Görlich, 2002). The effect of low-affinity importin-β binding on NPC topology is plotted in Fig. 3. With one obvious exception (I178D), NPC diameter is not significantly altered by any of the importin-β constructs tested. The isoleucine at position 178 of importin-β is essential for normal binding of FG-repeats (Bayliss et al., 2000). Replacing this Isoleucine (I) with an Aspartic acid (D) decreases the hydrophobic character of the FG binding region of importin-β and reduces binding affinity significantly. Nevertheless, despite

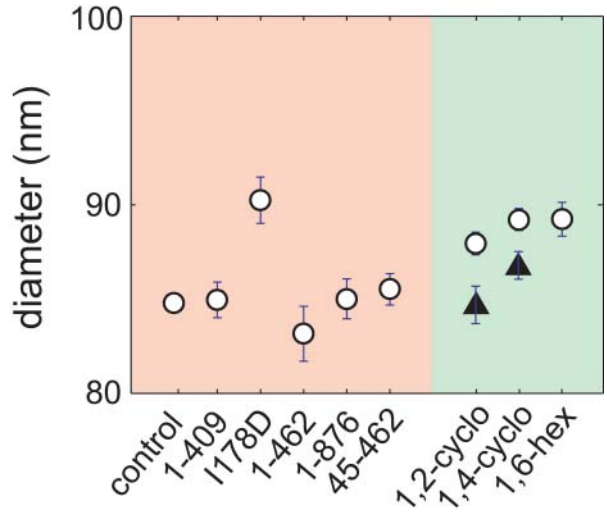

FIGURE 3 NPC diameter increases after incubation with molecules that bind with low affinity to FG-repeats. Plot of NPC diameter under the given conditions. NPC diameter increases after low affinity binding to FG-repeats by I178D (1 μM; 2 min), 1,2-cyclohexanediol (2.0%; 2–10 min), 1,4-cyclohexanediol (2.0%; 2–10 min) and 1,6-hexanediol (2.0%; 2–10 min). The solid triangles represent the extent of reversion in NPC diameter after washing out of 1,2- and 1,4-cyclohexandiol for 10 min. Washing involves prolonged handling of the nuclei as is evidenced by the increase in the size of the error bars representing the greater variability in NPC dimensions. The sample sizes are identical to those in Fig. 2 with the additions of 1,2-cyclohexanediol wash (85/2/2) and 1,4-cyclohexanediol wash (162/3/2).

a reduction in binding affinity, the I178D mutation has been shown to actually accentuate NPC transport (U. Kutay, unpublished result; also Bayliss et al., 2000). Interestingly, the I178D mutation when introduced into either the 45-462 or full-length importin-β background causes the NPC to dilate without affecting central channel depth (see Fig. 2).

Amphipathic alcohols have been previously demonstrated to reversibly collapse the permeability barrier of NPCs (Ribbeck and Görlich, 2002). Interestingly, in our measurements the amphipathic alcohols 1,2-cyclohexanediol, 1,4-cyclohexanediol and 1,6-hexanediol all increase NPC diameter (Fig. 2). The increase in NPC diameter with amphipathic alcohols was also largely invariant with incubation times $>$10 min. Furthermore, NPC diameter reverted to control values after the removal of the alcohols, which also testifies to the specificity of the effect. The solid triangles in Fig. 3 depict the extent of reversion of NPC diameter after removal of 1,2-cyclohexanediol and 1,4-cyclohexanediol for 10 min. It thus appears that weak FG-binding agents increase NPC diameter irrespective of whether they are endogenous (I178D importin-β constructs) or exogenous (amphipathic alcohols) in nature. This effect on NPC diameter might be correlated with the increase in cargo partitioning capacity previously observed with these agents (Ribbeck and Görlich, 2002).

It has been speculated that hydrophobic interactions are necessary to establish macromolecular transport through the NPC (Ribbeck and Görlich, 2002). These interactions would be mediated by repeating FG motifs that line the translocation pathway through the NPC and the hydrophobic characteristics of the transport receptors that contact them. Furthermore, these hydrophobic interactions must be carefully balanced because high-affinity interactions, while conferring increased specificity, would also slow transport rates. Our results could represent a physical manifestation of this interplay between FG-binding affinity and transport rates.

Thus far two nucleoporin FG motifs have been identified, xFxFG and GLFG, where x is either a serine, glycine, or alanine residue. Current evidence suggests that GLFG repeats might play a predominant role in nuclear export pathways (Powers et al., 1997). Furthermore, xFxFG repeats are a major component of the flexible cytoplasmic filaments that extend from the main body of the NPC and in this capacity possibly function as initial docking sites for cargo in line for passage through the NPC (Rout et al., 2000). If the FG-repeats within the lumen of the NPC are likewise filamentous then it is feasible that opposing FG-repeats might make weak hydrophobic contacts with each other interspersed by hydrophilic spaces formed by the linker sequences between repeats (Ribbeck and Görlich, 2001). Indeed, the density of FG-repeats has been estimated at nearly 10^4 per NPC, which might be conducive to such an arrangement of FG-repeats within the lumen of the NPC (Ribbeck and Görlich, 2002; Bayliss et al., 1999).

Several models have been put forward to explain nuclear transport. Most incorporate as a pivotal step in the translocation process the interaction between transport receptors and FG-repeats of the NPC (Rabut and Ellenberg, 2001). Points of contention between the different models center around the nature of the interaction between transport receptors and FG-repeats. In the selective phase model, a cargo's ability to transverse the lumen of the NPC is determined by its ability to selectively compete for the interactions between FG-repeats and thusly partition through the hydrophobic phase formed by interacting FG-repeats (Ribbeck and Görlich, 2001). Other models, by contrast, propose that NPC FG-repeats function as binding sites situated throughout the translocation pathway and that cargo size is restricted by the physical dimensions of the pore's central channel pathway (Rout et al., 2000). SFM analysis of NPC topology cannot unequivocally distinguish between these different models of nuclear transport. Within the framework of the selective phase model, however, our results might explain how amphipathic alcohols could dilate the lumen of the NPC by interfering with the putative labile interactions between FG-repeats. Through such a mechanism amphipathic alcohols might cause NPC dilation if tension exists within the plane of the nuclear envelope that is normally compensated by the binding forces between FG-repeats. The finding that these same amphipathic molecules increase the exclusion cutoff of NPCs initially supports this supposition (Ribbeck and Görlich, 2002). Interestingly, we found that all the amphipathic alcohols tested gave comparable degrees of NPC dilation suggesting a physical limit to dilation. This aspect of our study differed from previous biochemical results (Ribbeck and Görlich, 2002) demonstrating an effect on nuclear transport that was graded in reference to amphipathic character of the alcohol. On the other hand, an alternative interpretation of the data might be that these small polar alcohols alter the nuclear envelope in such a way as to allow larger than normal macromolecules to enter the nucleus independently of interfering with hydrophobic interactions within the lumen of the NPC. Such a nonspecific mechanism of action, however, would still need to be reconciled with the finding that amphipathic alcohols are without effect in the presence of wheat germ agglutinin, which implies that macromolecular entry takes place via the NPC and that the integrity of the nuclear envelope is not compromised by the alcohol treatment (Ribbeck and Görlich, 2002). Therefore, although our data may have implications for several models of nuclear transport they might nevertheless explain how interruption of intermolecular interactions within the lumen of the pore gives rise to NPC dilation.

Importin-β, one of the best-understood transport receptors, simultaneously interacts with cargo (via importin-α) and FG-repeats on passage through the NPC. Ran-GTP binding is essential for dissociation of the import complex from the NPC and consequently for functional termination of the transport process (Görlich et al., 1996). Kutay et al.

(1997) previously showed that truncating the Ran-GTP binding domain of importin-β causes its irreversible binding to the NPC with subsequent inhibition of nuclear transport. Our results suggest that transport block by the 45-462 mutant results from the occupation of available FG-binding sites (Fig. 1, *C–G*), implicating steric hindrance of further binding, rather than conformational changes in NPC structure. Furthermore, the I178D mutation in the context of the 45-462 mutant produced no change in NPC vertical aspect supporting the notion that unbinding from FG containing nucleoporins is mediated by Ran (see our unpublished result).

CONCLUSION

Our experimental data might indicate that we are observing two closely related, but mechanistically separable forms of transport modulation through the NPC. On the one hand, tight binding of importin-β mutants to FG-repeats increases the vertical aspect of the NPC in a manner that might explain the dominant negative transport block previously ascribed to these mutant transport receptors (Kutay et al., 1997). On the other hand, amphipathic molecules might interfere with the interaction of lumenal FG-repeats thereby increasing NPC diameter and accounting for the breakdown in selectivity observed with these molecules (Ribbeck and Görlich, 2002). Our experiments thus establish an important link between different experimental approaches aimed at understanding nuclear transport processes. In particular we demonstrate that topographic information obtained from SFM imaging is in accordance with previous scenarios deduced from purely biochemical experiments. Some of the observed features, such as an increase in pore diameter upon exposure to the I178D mutant, require an explanation beyond the scope of the current biochemical models accounting for nuclear transport.

We thank H. Murer and J. Biber for providing the oocytes for the initial experiments.

Financial support from ETH Zurich is acknowledged.

REFERENCES

Bayliss, R., K. Ribbeck, D. Akin, H. M. Kent, C. M. Feldherr, D. Görlich, and M. Stewart. 1999. Interaction between NTF2 and xFxFG-containing nucleoporins is required to mediate nuclear import of RanGDP. *J. Mol. Biol.* 293:579–593.

Bayliss, R., T. Littlewood, and M. Stewart. 2000. Structural basis for the interaction between FxFG nucleoporin repeats and importin-beta in nuclear trafficking. *Cell.* 102:99–108.

Danker, T., and H. Oberleithner. 2000. Nuclear pore function viewed with atomic force microscopy. *Pflugers Arch.* 439:671–681.

Finlay, D. R., and D. J. Forbes. 1990. Reconstitution of biochemically altered nuclear pores: transport can be eliminated and restored. *Cell.* 60:17–29.

Franco-Obregón, A., H. W. Wang, and D. E. Clapham. 2000. Distinct ion channel classes are expressed on the outer nuclear envelope of T- and B-lymphocyte cell lines. *Biophys. J.* 79:202–214.

Görlich, D., and U. Kutay. 1999. Transport between the cell nucleus and the cytoplasm. *Annu. Rev. Cell Dev. Biol.* 15:607–660.

Görlich, D., N. Panté, U. Kutay, U. Aebi, and F. R. Bischoff. 1996. Identification of different roles for RanGDP and RanGTP in nuclear protein import. *EMBO J.* 15:5584–5594.

Grote, M., U. Kubitscheck, R. Reichelt, and R. Peters. 1995. Mapping of nucleoporins to the center of the nuclear pore complex by post-embedding immunogold electron microscopy. *J. Cell Sci.* 108:2963–2972.

Jäggi, R. D., A. Franco-Obregón, P. Studerus, and K. Ensslin. 2001. Detailed analysis of forces influencing lateral resolution for Q-control and tapping mode. *Appl. Phys. Lett.* 79:135–137.

Jäkel, S., and D. Görlich. 1998. Importin beta, transportin, RanBP5 and RanBP7 mediate nuclear import of ribosomal proteins in mammalian cells. *EMBO J.* 17:4491–4502.

Kutay, U., E. Izaurralde, F. R. Bischoff, I. W. Mattaj, and D. Görlich. 1997. Dominant-negative mutants of importin-beta block multiple pathways of import and export through the nuclear pore complex. *EMBO J.* 16:1153–1163.

Oberleithner, A., E. Brinckmann, A. Schwab, and G. Krohne. 1994. Imaging nuclear pores of aldosterone-sensitive kidney cells by atomic force microscopy. *Proc. Natl. Acad. Sci. USA.* 91:9784–9788.

Perez-Terzic, C., J. Pyle, M. Jaconi, L. Stehno-Bittel, and D. E. Clapham. 1996. Conformational states of the nuclear pore complex induced by depletion of nuclear Ca2+ stores. *Science.* 273:1875–1877.

Powers, M. A., D. J. Forbes, J. E. Dahlberg, and E. Lund. 1997. The vertebrate GLFG nucleoporin, Nup98, is an essential component of multiple RNA export pathways. *J. Cell Biol.* 136:241–250.

Rabut, G., and J. Ellenberg. 2001. Nucleocytoplasmic transport: diffusion channel or phase transition? *Curr. Biol.* 11:R551–R554.

Radu, A., M. S. Moore, and G. Blobel. 1995. The peptide repeat domain of nucleoporin Nup98 functions as a docking site in transport across the nuclear pore complex. *Cell.* 81:215–222.

Ribbeck, K., and D. Görlich. 2002. The permeability barrier of nuclear pore complexes appears to operate via hydrophobic exclusion. *EMBO J.* 21: 2664–2671.

Ribbeck, K., and D. Görlich. 2001. Kinetic analysis of translocation through nuclear pore complexes. *EMBO J.* 20:1320–1330.

Rout, M., J. Aitchison, A. Suprapto, K. Hjertaas, Y. Zhao, and B. Chait. 2000. The yeast nuclear pore complex: composition, architecture, and transport mechanism. *J. Cell Biol.* 148:635–651.

Stewart, M. 2000. Insights into the molecular mechanism of nuclear trafficking using nuclear transport factor 2 (NTF2). *Cell Struct. Funct.* 25:217–225.

Stoffler, D., K. N. Goldie, B. Feja, and U. Aebi. 1999. Calcium-mediated structural changes of native nuclear pore complexes monitored by time-lapse atomic force microscopy. *J. Mol. Biol.* 287:741–752.

Wang, H., and D. E. Clapham. 1999. Conformational changes of the in situ nuclear pore complex. *Biophys. J.* 77:241–247.